International Journal of Electrical and Computer Engineering (IJECE)
Vol. 13, No. 4, August 2023, pp. 3805~3816
ISSN: 2088-8708, DOI: 10.11591/ijece.v13i4.pp3805-3816

Direct torque control and dynamic performance of induction motor using fractional order fuzzy logic controller

Geeta Kamalapur, Mruttanjaya S. Aspalli
Department of Electrical and Electronics Engineering, Poojya Doddappa Appa College of Engineering, Kalaburagi, India

Article Info

Article history:

Received May 14, 2022
Revised Nov 6, 2022
Accepted Nov 26, 2022

Keywords:

Direct torque control
Fractional order fuzzy logic controller
Fuzzy logic controller
Induction motor
MATLAB/Simulink

ABSTRACT

Conventional direct torque control (DTC) is one of the best control systems for regulating the torque of an induction motor (IM). However, the DTC's enormous waves in flux and torque cause acoustic noise that degrades control performance, especially at low speeds due to the DTC's low switching frequency. Direct torque control systems, which focus just on torque and flux, have been proposed as a solution to these problems. In order to improve DTC control performance, this work introduces a fractional-order fuzzy logic controller method. The objective is to analyze this technique critically with regard to its efficacy in reducing ripple, its tracking speed, its switching loss, its algorithm complexity, and its sensitivity to its parameters. Simulation in MATLAB/Simulink verifies the anticipated control approach's performance.

Corresponding Author:

Geeta Kamalapur
Department of Electrical and Electronics Engineering, Poojya Doddappa Appa College of Engineering
Kalaburagi, Karnataka, India
Email: geeta.u.kamalapur@gmail.com

1. INTRODUCTION

Takahashi and Noguchi proposed direct torque control (DTC) for AC machines in 1986 [1]. In comparison to the field orientating control (FOC) technique, DTC has attracted aid of multiple academics since its several benefits, including its simple structure, quick dynamic reaction, and lower reliance on machine parameters. Dynamic variation performance are the primary issues with traditional DTCs [2]–[4]. The presence of hysteresis device in the standard DTC scheme [5] is well established as the action of switch frequency changes. Several solutions have been proposed to alleviate DTC limitations, such as using artificial intelligence (AI) algorithms [6]–[8]. Several academics have proposed and developed the space vector modulation (SVM) technique to eliminate torque and flux ripples by operating the inverter at a continuous switching frequency. To calculate reference voltage vector components that are adjusted by the SVM unit to produce inverter switching states, the SVM-DTC replaces two hysteresis controllers with two proportional integral (PI) controllers [9]. In terms of ripples, this control approach increases DTC performance. The usage of PI controllers, on the other hand, necessitates a thorough understanding of the controlled system's specific model [10], [11].

Furthermore, selecting controller gains is a difficult task. In most cases, gain values calculated using simulation do not perform well in practice. When interruptions, uncertainty, and parameter change are present, PI controllers have limited functionality. As a consequence, the system's dynamic and stability will be justified [12], [13]. To overcome the restrictions of the refereed methods, strong nonlinear control systems for induction motor control, such as the fuzzy logic controller (FLC) [12], have been developed. The initial contribution of this study is the implementation of a FLC for an induction motor, which is motivated by the discussion above. This controller was chosen because of its ease of use and minimal cost of implementation [14], [15]. Figure 1 depicts the block diagram of fractional order FLC based DTC of the induction motor.

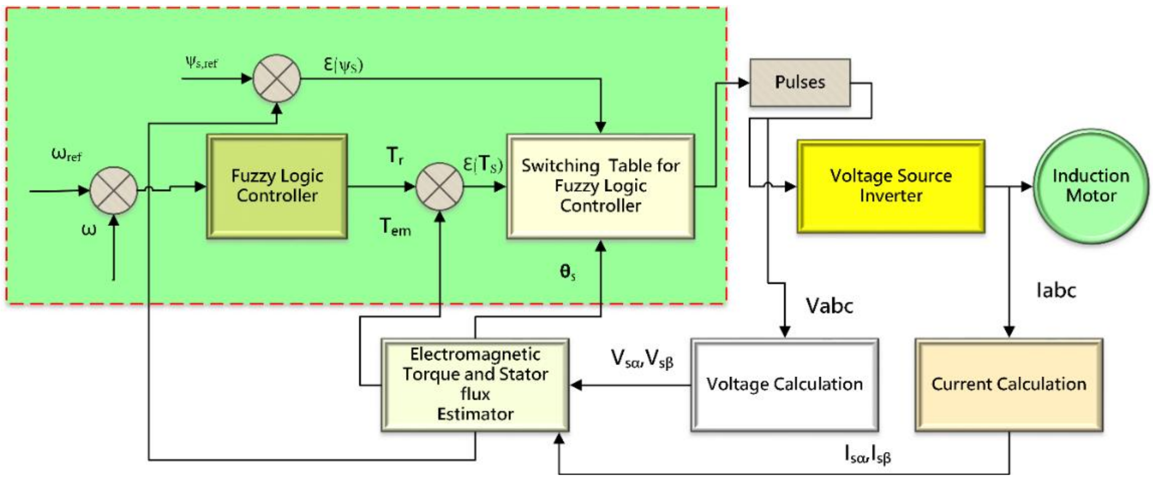

Figure 1. Block diagram of fractional order fuzzy logic controller (FOFLC) based DTC of the induction machine

2. DYNAMIC MODELING OF INDUCTION MOTOR

To model the three-phase induction motor, certain assumptions are made: each stator winding is distributed along the air gap to bring out sinusoidal mmf [16]. The rotor has a squirrel cage shape, and the airspace between both the machines is consistent. Coils are the same in both cases. The losses due to stator winding saturation, hysteresis, and eddy currents are not considered [17], [18]. Indeed, the induction motor's dynamic behavior in the stationary action (α, β) defined as below. In the stationary reference (α, β), the stator voltage vector V_s is represented by (1), (2), (3):

$$V_{s\alpha} = \frac{d\phi_{s\alpha}}{dt} + R_{s i_{s\alpha}} \tag{1}$$

$$V_{s\beta} = \frac{d\phi_{s\beta}}{dt} + R_s i_{s\beta} \tag{2}$$

$$\overline{V_s} = \frac{d\overline{\phi_s}}{dt} + R_s \overline{\iota_s} \tag{3}$$

where ($V_{s\alpha}$, $V_{s\beta}$), ($\phi_{s\alpha}$, $\phi_{ss\beta}$), and ($i_{s\alpha}$, $i_{s\beta}$) are the voltage, stator flux, and stator current components in the concordant reference (alpha, beta), respectively. The stator resistance is denoted by Rs. In the concordance reference (α, β), the time derivative of the rotor flow is as (4), (5):

$$\frac{d\phi_{\{r\alpha\}}}{dt} = -\mathrm{R}_{\{\mathrm{r}\}\mathrm{i}_{\{r\alpha\}}} - \omega_{\{\mathrm{m}\}\phi_{\{\mathrm{r}\beta\}}} \tag{4}$$

$$\frac{d\phi_{\{r\beta\}}}{dt} = -R_{\{r\}i_{\{r\beta\}}} - \omega_{\{m\}\phi_{\{r\alpha\}}} \tag{5}$$

where $(\phi_{r\alpha}, \phi_{r\beta})$ and $(i_{r\alpha}, i_{r\beta})$ are the flux and current components of the rotor, respectively. The rotor resistance and motor speed are represented by R_r and ω_m, respectively. The components of the stator flux vector ϕ_s can be represented as (6), (7), (8):

$$\phi_{\{s\alpha\}} = L_{\{s\}i_{\{s\alpha\}}} + \mathrm{M}i_{\{r\alpha\}} \tag{6}$$

$$\phi_{s\beta} = L_s i_{s\beta} + M i_{r\beta} \tag{7}$$

$$\overline{\phi_s} = L_s \overline{\iota_s} + M \overline{\iota_r} \tag{8}$$

The flux vector of the stator ϕ_s and its elements can be represented as (9), (10), (11):

$$\phi_{r\alpha} = L_r i_{r\alpha} + M i_{s\alpha} \tag{9}$$

$$\phi_{r\beta} = L_r i_{r\beta} + M i_{s\beta} \tag{10}$$

$$\overline{\phi_r} = L_r \overline{i_r} + M \overline{i_s} \tag{11}$$

The stator, rotor, and mutual inductance are represented by L_s, L_r, and *M*, respectively. The following is a brief description of mechanical motor movements.

$$J \frac{dohm_m}{dt} = T_{em} - T_l - fohm_m \tag{12}$$

The torque, the load torque, rotor momentum, and viscous frictional force are represented as *T_{em},$T {l}$ J* and *f*, respectively. The motor's electromagnetic torque can be calculated using the formula (13).

$$T_{em} = \frac{3}{2} N_p \left(\phi_{s\alpha} i_{s\beta} - \phi_{s\beta} i_{s\alpha} \right) \tag{13}$$

The pole pairs are denoted by N_p. The state model of the induction motor is described by the time derivative of the stator current and flux components, as shown (14), (15), (16), (17).

$$\frac{di_{s\alpha}}{dt} = -\frac{1}{\sigma}\left(\frac{1}{T_r} + \frac{1}{T_s}\right) i_{s\alpha} - \omega_m i_{s\alpha} + \frac{1}{\sigma L_s T_r} \phi_{s\alpha} + \frac{\omega_m}{\sigma L_s} \phi_{s\beta} + \frac{1}{\alpha L_s} v_{s\alpha} \tag{14}$$

$$\frac{di_{s\beta}}{dt} = -\frac{1}{\sigma}\left(\frac{1}{T_r} + \frac{1}{T_s}\right) i_{s\beta} - \omega_m i_{s\beta} + \frac{1}{\sigma L_s T_r} \phi_{s\beta} + \frac{\omega_m}{\sigma L_s} \phi_{s\alpha} + \frac{1}{\beta L_s} v_{s\beta} \tag{15}$$

$$\frac{d\phi_{s\alpha}}{dt} = v_{s\alpha} + R_s i_{s\alpha} \tag{16}$$

$$\frac{d\phi_{s\beta}}{dt} = v_{s\beta} + R_s i_{s\beta} \tag{17}$$

3. CONTROL METHOD

3.1. Design of field orientating control

The FOC is very much famous to understand the derivative operator. The numerical expression for fractional order proportional integral (FOPI) is

$$c(s) = kp + \frac{Ki}{s^{\lambda}} \tag{18}$$

λ is range of (0,1). If *$\lambda$$\geq$2* is transformed to high-order expression is equal to PI controller. The F.O is described in (18) is common character of PI controller. To resolve the issues in fractional order fuzzy logic (FOFL) controller the effective filters can be used. The fitting range is (*ω_{b},ω_{h}*). The function of fractional order is

$$K(s) = \left[\frac{1+\frac{as}{b\omega_a}}{1+\frac{bs}{b\omega_h}}\right]^{\lambda} \tag{19}$$

where $0 \leq \lambda \leq 1;\ s = j\omega, a \geq 0;\ b \geq 0$, and

$$K(s) = \left(\frac{as}{b\omega_a}\right)^{\lambda} \left(1 + \frac{-bs+b}{bs^2 + a\omega_h s}\right)^{\lambda} \tag{20}$$

In the frequency range $\omega_b \geq \omega \geq \omega_h$ by using a "Taylor- series" expansion, we obtain

$$K(s) = \left(\frac{as}{b\omega_a}\right)^{\lambda} \left(1 + (s) + \frac{\lambda(\lambda-1)}{2} P^2(s) \ldots.. \right) \tag{21}$$

where

$$F(s) = \left(1 + \frac{-bs+b}{bs^2+a\omega_h s}\right) \tag{22}$$

It is then found that

$$s^\lambda = \frac{(b\omega_a)^\lambda a^\lambda}{a^\lambda\left(1+(s)+\frac{\lambda(\lambda-1)}{2}P^2(s).....\right)}\left(\frac{1+as/b\omega_a}{1+bs/b\omega_b}\right)^\lambda \tag{23}$$

it leads to

$$s^\lambda = \frac{(b\omega_a)^\lambda a^\lambda}{a^\lambda(1+\lambda P(s))}\left(\frac{1+as/b\omega_a}{1+bs/b\omega_b}\right)^\lambda. \tag{24}$$

Thus, the FOC is defined as (25).

$$s^\lambda \approx \left(\frac{(b\omega_a)}{b}\right)^\lambda \left(\frac{ds^2+b\omega_h s}{d(1-\lambda)s^2+b\omega_h s+d\lambda}\right)\left(\frac{1+bs/d\omega_b}{1+ds/d\omega_h}\right)^\lambda \tag{25}$$

As shown in (21) is proportionate when all the poles are on LHS of s-plane. The poles should follow the stability condition.

$$b(1-\lambda)s^2 + a\omega_h s + b \tag{26}$$

Hence, all the poles of (24) are stable within the limit of (ω_l, ω_h).

$$K(s) = \lim N \to \infty F_N(s) = \prod_F^N \lim N \to \infty = -N\frac{1+s/\omega_k'}{1+s/\omega_k} \tag{27}$$

According to the algorithmic distribution of real zeros and poles, the zero and pole of rank k can be written as (28).

$$\omega_k' = \left(\frac{b\omega_a}{a}\right)^{\frac{\lambda-2k}{2N+1}}, \omega_k = \left(\frac{b\omega_b}{a}\right)^{\frac{\lambda+2k}{2N+1}} \tag{28}$$

Hence final model can be stated as (29).

$$s^\lambda \approx \left(\frac{(b\omega_a)}{b}\right)^\lambda \left(\frac{ds^2+b\omega_h s}{d(1-\lambda)s^2+b\omega_h s+d\lambda}\right) = -N\frac{1+s/\omega_k'}{1+s/\omega_k} \tag{29}$$

The negative poles in real part for $0 \leq \lambda \leq 1$. The poles in (27) is in range of(ω_l/ω_h). The (27) is approximated by uninterrupted -time coherent simulation. It is configured and ordered in the system depicts in Figure 2.

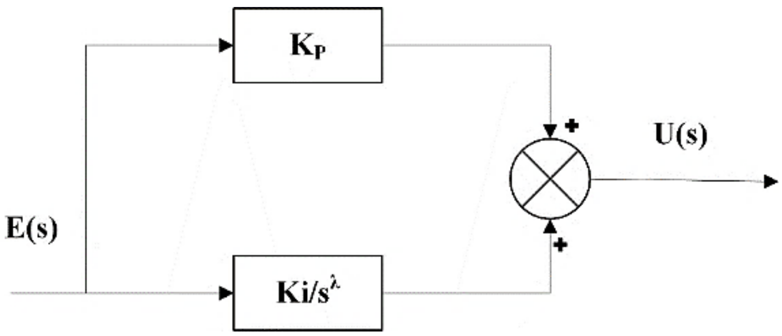

Figure 2. Structure of FOPI controller

3.2. Design of fuzzy logic controller

A simple FLC's base level is seen in Figure 3. FLC is made up of input and output variables, as well as fuzzy inference, defuzzification, and fuzzification rules [19]–[21]. The FLC block diagram is shown in Figure 3. Seven membership functions are used to construct the fuzzy sets. A membership function for generating a fuzzy set is selected and created. Figure 4(a) and (b) depicts a FIS with inputs error and error change. Figure 5(a) and (b) depicts the output membership functions ΔKp and ΔKi. In order to improve the inference [22]. Figure 6 depicts the FOFL controller's construction. Figure 7 depicts a proposed control technique with a new FOFL.

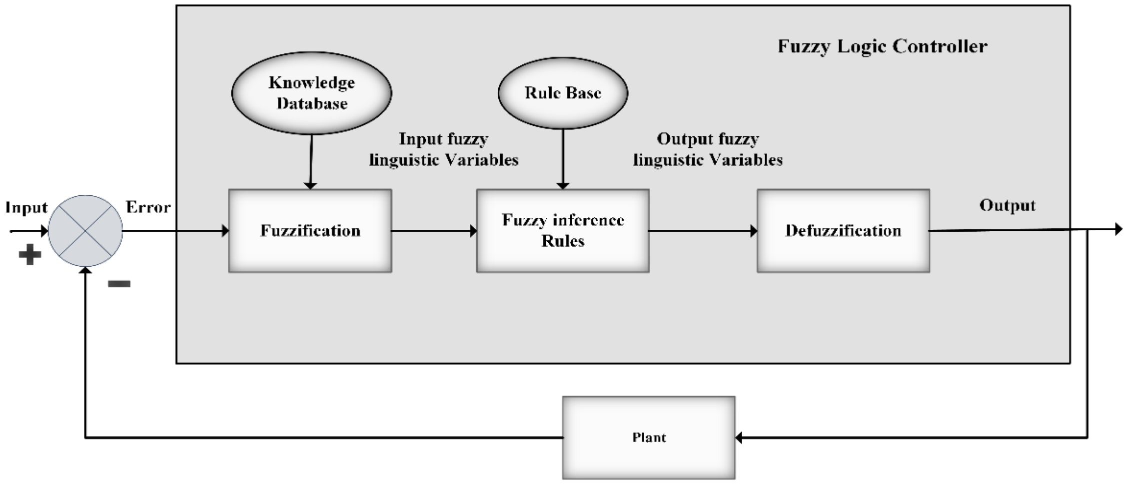

Figure 3. Structure of FL controller

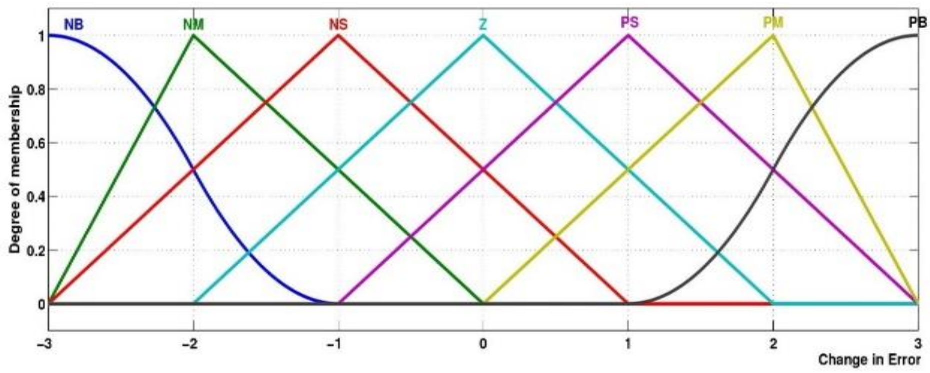

(a)

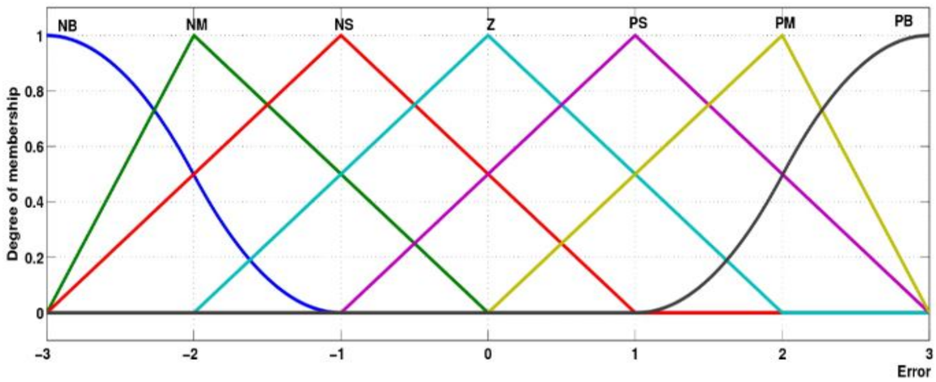

(b)

Figure 4. Membership functions of error and change in error (a) membership functions of error and (b) membership functions of CE

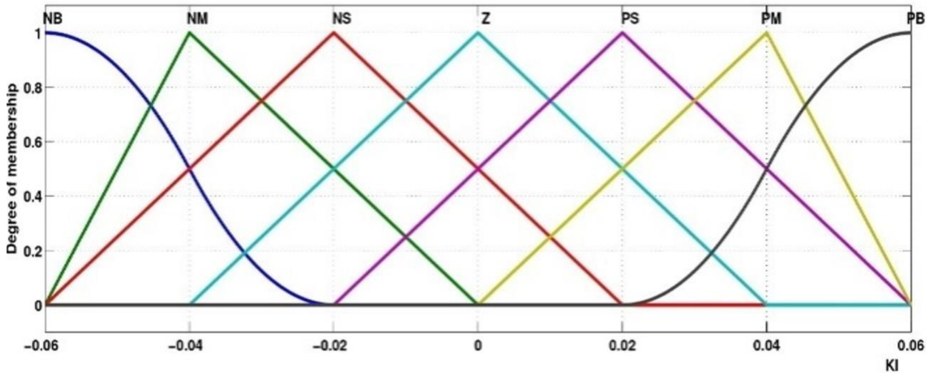

(a)

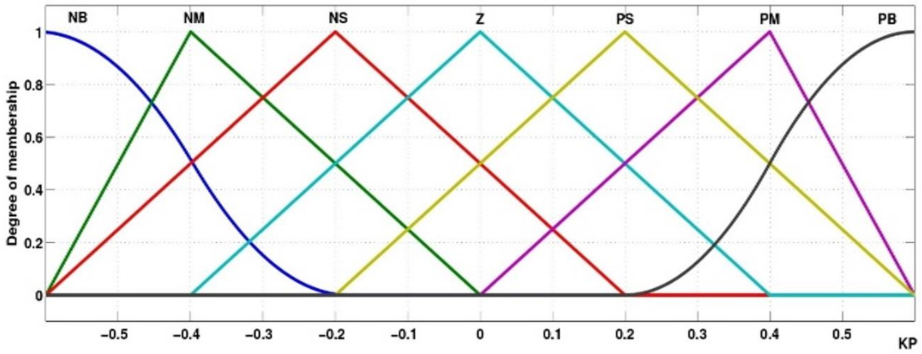

(b)

Figure 5. Membership functions of adjusted gains (a) membership functions of Δki and (b) membership functions for ΔKp

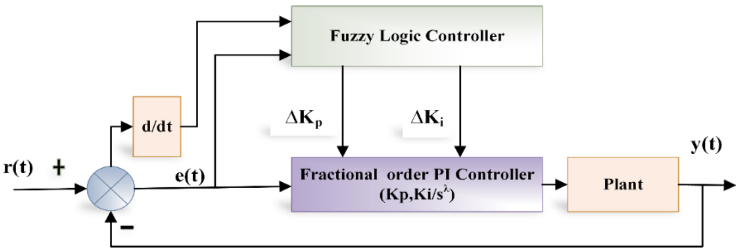

Figure 6. Design of proposed FOFLC

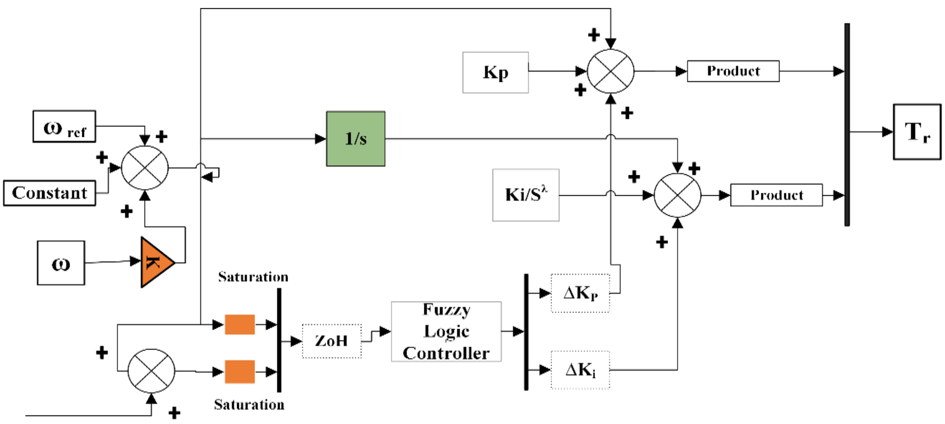

Figure 7. Control strategy of FOFLC

4. LEARNING PART

FLC works well in closed loop feedback systems, especially whenever the i/p and o/p are non-linear. Input errors and a gain value for the K_p and K_i terms are used by classical controllers like FOC [23], [24]. As a result, the controller action falls short of the standard for complex, non-linear systems. Instead of a fixed gain, the dynamic gain value for the K_p, complete terms, and derivates might be used. Changing a FOPI control structure's dynamic gain enhances controller's performance and quickly remains stable system output during variance and noise. In light of these issues, an FLC system with a FOC is proposed [25]. The FOFL system incorporates the FLC and FOF controller's functionality. The FLC is set up in this controller scheme to calculate the proportional scale factor 'E' using the system error and error derivatives as inputs'[9]. In full, these scale factors will be used to change the amount of controller gain in each sample interval. The structure of FOFL control mechanism is seen in Figure 8 [5]. FLC creates the multiplier for proportional and integral terms using error and its derivative in the proposed system of control, and these values are then utilized to update the FOFL controller's gain settings. The K_P and K_I signal gain levels for the FOFL controller are estimated using the calculations in (30), (31).

$$K_P = k_p + \Delta K_p \tag{30}$$

$$K_I = k_i + \Delta k_i \tag{31}$$

Here k_p and k_i are the determinate gain values. The flowchart of the planned method is depicted in Figure 8.

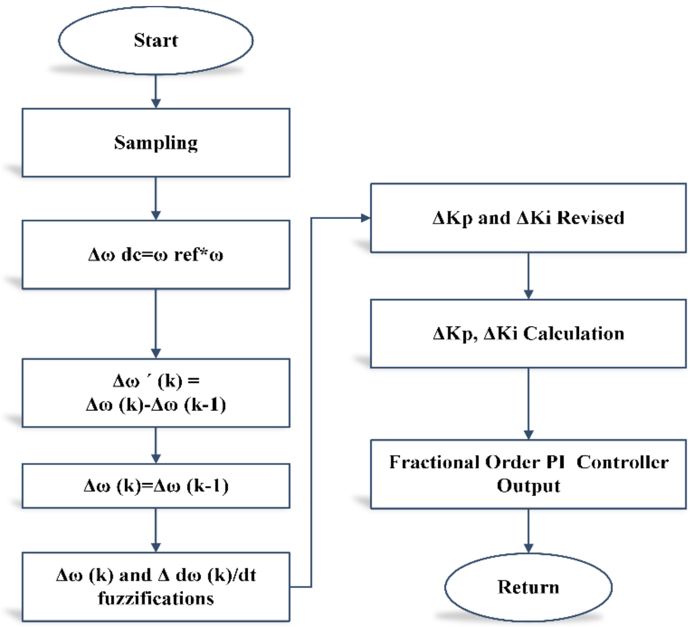

Figure 8. Flowchart for proposed system

5. RESULTS AND DISCUSSION

MATLAB/Simulink was used to do dynamic modelling and simulation of a three-phase induction motor. The model was put to the test for two different induction motor ratings: low and high. And also, it examined No load conditions, constant load condition and variable load conditions. The results are discussed in the following cases.

5.1. At no load conditions

Figure 9 shows the torque and speed characteristics of the PI and FOFLC. The speed and torque parameters of traditional PI and FLC are shown in Figure 9. When the FOFLC is added to the simulation model and both results are taken at the same time, it appears that the rising time lowers. FOLC has a rise time of 0.3350 seconds, while PI has a rise time of 0.3435 seconds. There is a minor variation in T_r, M(overshoot), and T_s that is not visible in the graph. The torque and speed characteristics variation of IM for all controller is shown in Figures 10 and 11 respectively.

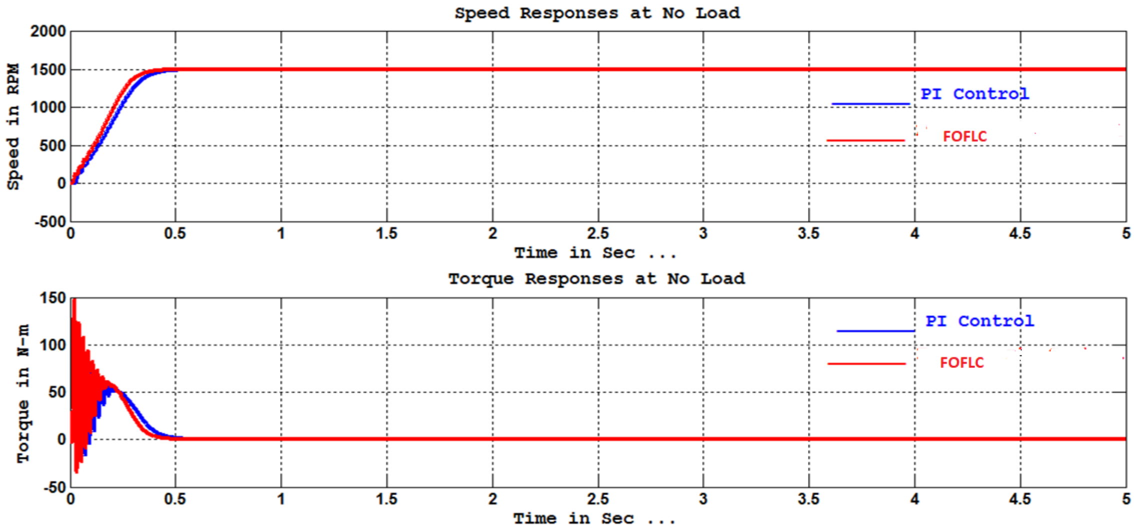

Figure 9. Torque and speed characteristics of PI and FOFL controller

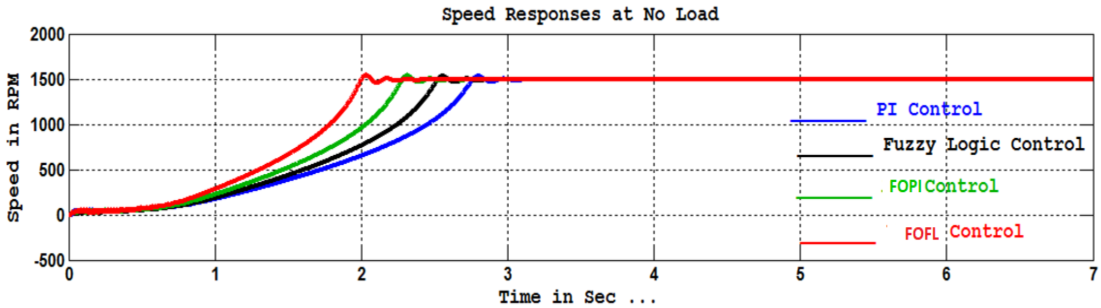

Figure 10. Speed characteristics of IM using all controllers

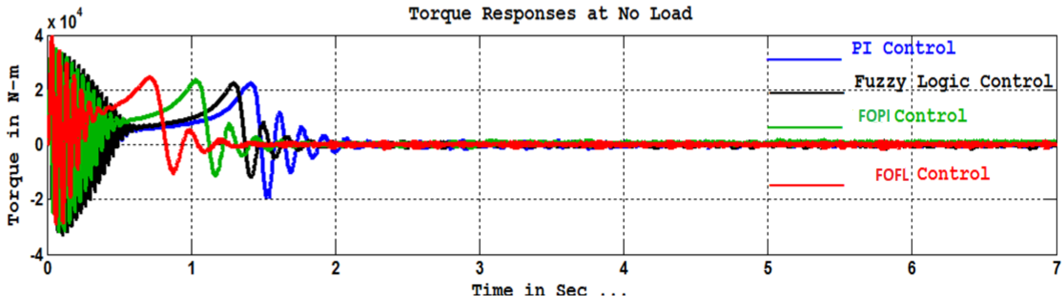

Figure 11. Torque characteristics of IM using all controllers

5.2. At constant load

The torque and speed parameters are shown in Figure 12. There is a drop in torque and speed when a 14 Nm load is applied rapidly at 1.5 sec. Following the occurrence of the initial transient, the motor settles at 1.9466 sec with the FOFL controller and 1.8787 sec with the PI controller. To make a fair comparison, the PI controller is tuned at rated circumstances. When the motor is started with a constant of 14 Nm, the simulated results are shown in Figure 10. The drive's performance in comparison to traditional PI and FOLC-based drive systems. When a constant load is applied suddenly, the PI controller takes longer to reach the desired speed than the fuzzy controller. The torque and speed characteristics variation of IM for all controller is shown in Figures 13 and 14 respectively.

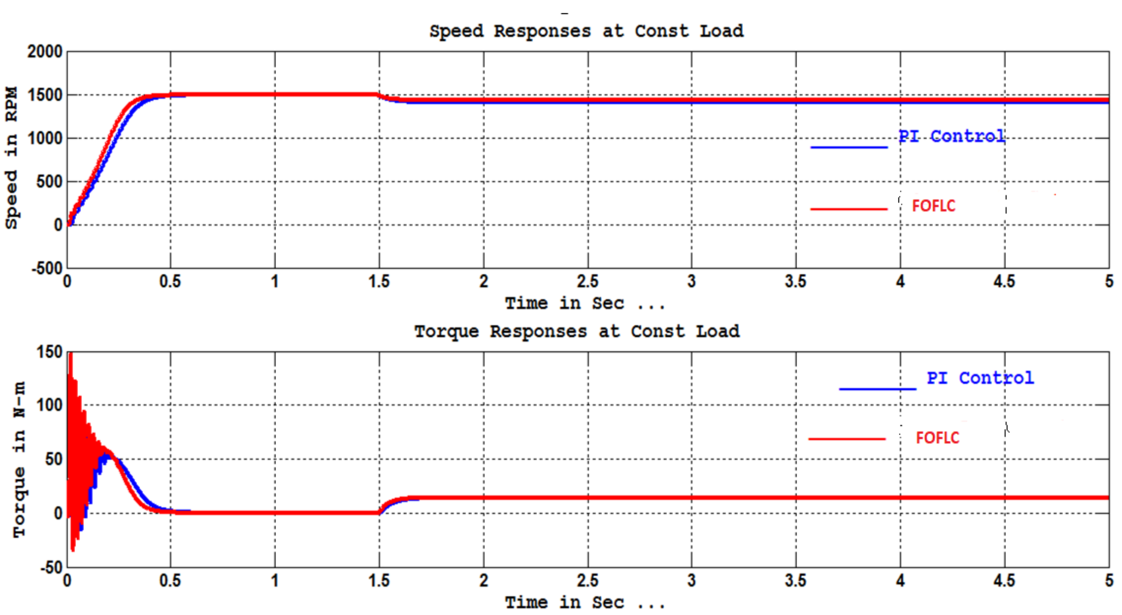

Figure 12. Torque and speed characteristics of PI and FOFL controller

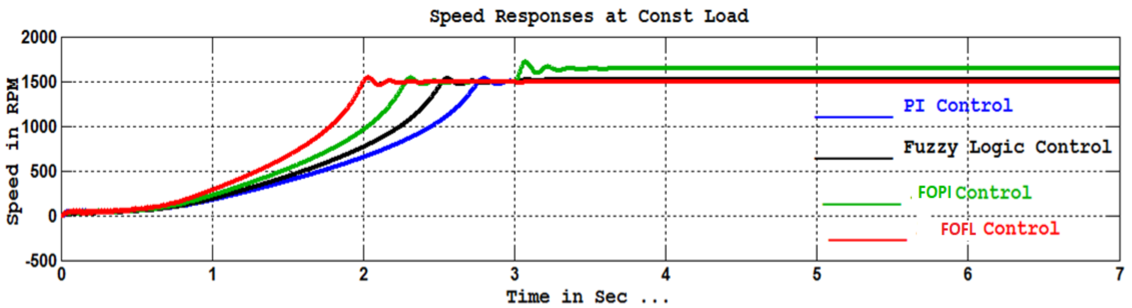

Figure 13. Speed characteristics of IM using all controllers

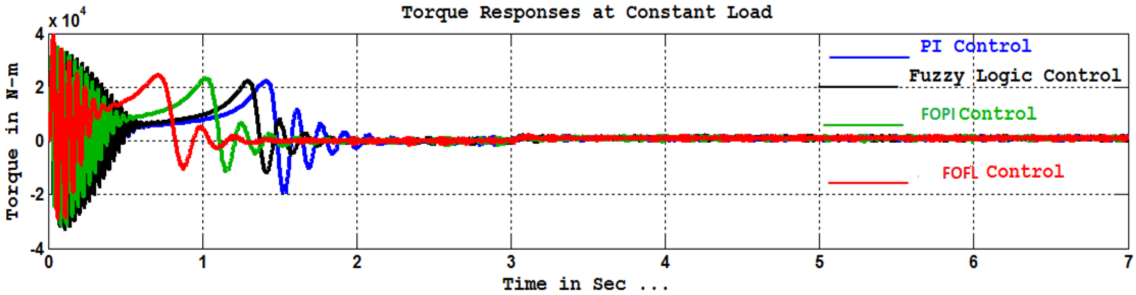

Figure 14. Torque characteristics of IM using all controllers

5.3. At variable load

When using a PI controller, the speed response peaks at 0.6 seconds, but when using a FOFL controller, the speed response is swift and smooth, as illustrated in Figure 15. Using a FOFL controller, the motor speed follows its reference with zero steady-state error and a quick reaction. The PI controller, on the other hand, exhibits steady-state inaccuracy when the initial current is high. It should be noted that the load conditions have an impact on the speed response. A PI controller with changeable operating circumstances has this disadvantage. In terms of rising time and steady state error, the FOFL controller outperforms. The torque and speed characteristics variation of IM for all controller is shown in Figures 16 and 17 respectively.

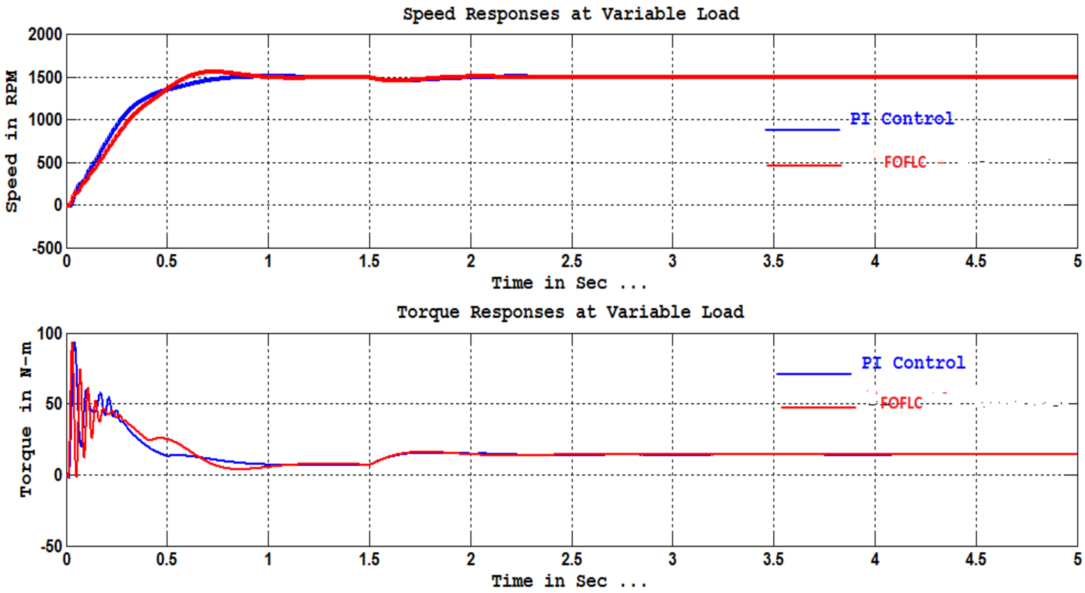

Figure 15. Torque and speed characteristics of PI and FOFL controller

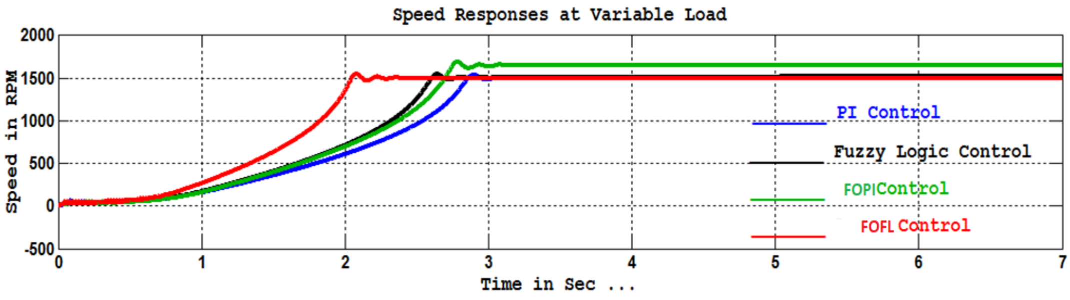

Figure 16. Speed characteristics of IM using all controllers

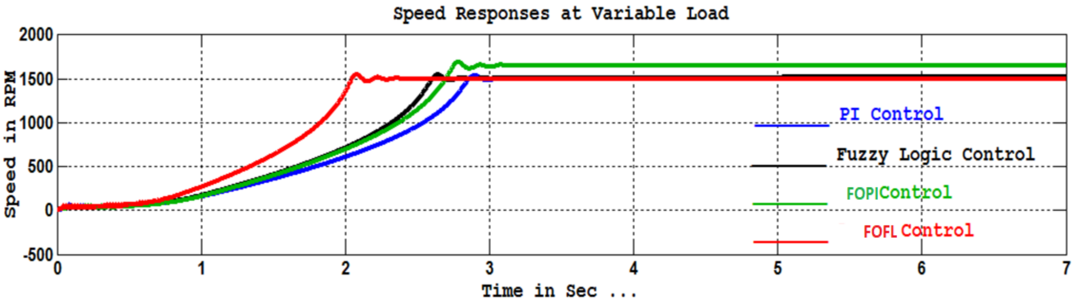

Figure 17. Torque Characteristics of IM using all controllers

Tables 1 and 2 compare the performance of PI and FOFL controllers during steady state and transient operation in terms of T_r, M(overshoot), and Ts for various load circumstances. The tables show that FOFLC has a faster rise time, settling time, and less overshoot than PI under various load circumstances. As a result, the FOFLC controller out performs the PI controller. This demonstrates the three-phase induction motor's ability to adjust speed and deliver a precise and fast reaction with no overshoot and no steady state inaccuracy. The current development of the stator is seen in Figures 18(a) and (b). The stator current in the FOFL controller-based IM has an excellent sinusoid waveform, but the stator current in the traditional DTC has significant harmonics.

Table 1. Dynamic performance comparison between PI and FOFLC during transient operation

Control strategies	Rise Time(sec)	%Overshoot	Settling Time (sec)
PI	0.3435	1.1793	0.5163
FLC	0.335	0.9454	0.4731
FOPI	0.2457	0.7018	0.3380
FOFL	0.2189	0.6059	0.2962

Table 2. Dynamic performance comparison between PI and FOFLC during transient operation

Control strategies	Rise Time(sec)	%Overshoot	Settling Time (sec)
PI	0.5516	0.629	1.9466
FLC	0.4825	0.5987	1.8787
FOPI	0.2873	0.4564	1.7641
FOFL	0.2641	0.4064	1.6423

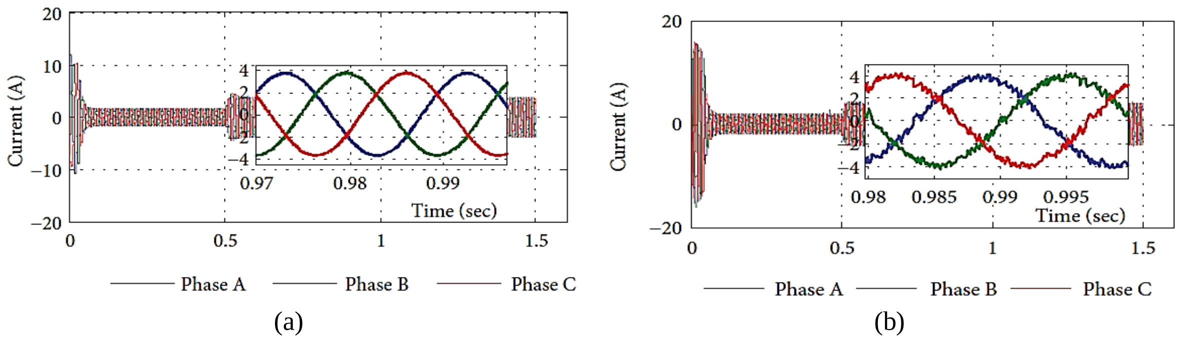

Figure 18. 3-ϕ stator current for 18 (a) traditional controller and 18 (b) FOFLC based on IM

6. CONCLUSION

MATLAB/Simulink software is used to model the closed loop control system of a FOFLC and a three-phase SVPWM VSI in this paper. It can be inferred that using FOFLC for various load conditions enhances and smooth's out motor torque and stator current ripples. The simulation findings proved the FOFL controller's excellent dynamic performance and robustness during the transient period and under abrupt loads. The proposed intelligent controller outperformed the parameter fixed PI controller, according to the results. In the case of a PI controller, more and more trial and error are required to achieve optimal speed control of an IM drive.

REFERENCES

[1] I. Takahashi and T. Noguchi, "Take a look back upon the past decade of direct torque control [of induction motors]," in *Proceedings of the IECON'97 23rd International Conference on Industrial Electronics, Control, and Instrumentation (Cat. No.97CH36066)*, vol. 2, pp. 546–551, doi: 10.1109/IECON.1997.671792.

[2] E. Himabindu, D. Krishna, and V. M. Gopala, "Performance of intelligent controller-based bearingless switched reluctance motor," in *Advances in Renewable Energy and Electric Vehicles*, Springer Singapore, 2022, pp. 355–373.

[3] J. Zhao and B. K. Bose, "Evaluation of membership functions for fuzzy logic controlled induction motor drive," in *IEEE 2002 28th Annual Conference of the Industrial Electronics Society. IECON 02*, 2002, vol. 1, pp. 229–234, doi: 10.1109/IECON.2002.1187512.

[4] M. Adamczyk and T. Orlowska-Kowalska, "Postfault direct field-oriented control of induction motor drive using adaptive virtual current sensor," *IEEE Transactions on Industrial Electronics*, vol. 69, no. 4, pp. 3418–3427, Apr. 2022, doi: 10.1109/TIE.2021.3075863.

[5] Y. Zahraoui, M. Akherraz, and S. Elbadaoui, "Fuzzy logic speed control and adaptation mechanism-based twelve sectors DTC to improve the performance of a sensorless induction motor drive," *International Journal on Electrical Engineering and Informatics (IJEEI)*, vol. 13, no. 3, pp. 508–529, Sep. 2021, doi: 10.15676/ijeei.2021.13.3.1.

[6] Z. Farooq, A. Rahman, and S. A. Lone, "System dynamics and control of EV incorporated deregulated power system using MBO-optimized cascaded ID-PD controller," *International Transactions on Electrical Energy Systems*, vol. 31, no. 11, Nov. 2021, doi: 10.1002/2050-7038.13100.

[7] F. Aymen, N. Mohamed, S. Chayma, C. H. R. Reddy, M. M. Alharthi, and S. S. M. Ghoneim, "An improved direct torque control topology of a double stator machine using the fuzzy logic controller," *IEEE Access*, vol. 9, pp. 126400–126413, Oct. 2021, doi: 10.1109/ACCESS.2021.3110477.

[8] B. Singh, R. Kumar, and P. Kant, "Adjustable speed induction motor drive fed by 13-level cascaded inverter and 54-pulse converter," *IEEE Transactions on Industry Applications*, vol. 58, no. 1, pp. 890–900, 2021.

[9] S. A. A. Tarusan, A. Jidin, and M. L. M. Jamil, "The optimization of torque ripple reduction by using DTC-multilevel inverter," *ISA Transactions*, vol. 121, pp. 365–379, Feb. 2022, doi: 10.1016/j.isatra.2021.04.005.

[10] C. P. Gor, V. A. Shah, and B. Rangachar, "Fuzzy logic based dynamic performance enhancement of five phase induction motor under arbitrary open phase fault for electric vehicle," *International Journal of Emerging Electric Power Systems*, vol. 22, no. 4, pp. 473–492, Aug. 2021, doi: 10.1515/ijeeps-2020-0271.

[11] S. R. Satpathy, S. Pradhan, R. Pradhan, R. Sahu, A. P. Biswal, and B. P. Ganthia, "Direct torque control of mathematically modeled induction motor drive using PI-Type-I fuzzy logic controller and sliding mode controller," in *Intelligent Systems*, Springer Singapore, 2021, pp. 239–251.

[12] I. Eke, M. Saka, H. Gozde, Y. Arya, and M. C. Taplamacioglu, "Heuristic optimization based dynamic weighted state feedback approach for 2DOF PI-controller in automatic voltage regulator," *Engineering Science and Technology, an International Journal*, vol. 24, no. 4, pp. 899–910, Aug. 2021, doi: 10.1016/j.jestch.2020.12.023.

[13] B. P. Ganthia, R. Pradhan, R. Sahu, and A. K. Pati, "Artificial ant colony optimized direct torque control of mathematically modeled induction motor drive using pi and sliding mode controller," in *Recent Advances in Power Electronics and Drives*, Springer Singapore, 2021, pp. 389–408.

[14] Z. Wang, W. Sun, and D. Jiang, "Stability analysis and trajectory design of a nonlinear switching system for speed sensorless induction motor drive," *IEEE Transactions on Industrial Electronics*, vol. 69, no. 6, pp. 5514–5524, Jun. 2022, doi: 10.1109/TIE.2021.3086712.

[15] B. Chikondra, U. R. Muduli, and R. K. Behera, "Improved DTC technique for THL-NPC VSI fed five-phase induction motor drive based on VVs assessment over a wide speed range," *IEEE Transactions on Power Electronics*, vol. 37, no. 2, pp. 1972–1981, 2021.

[16] Prince and A. S. Hati, "A comprehensive review of energy-efficiency of ventilation system using artificial intelligence," *Renewable and Sustainable Energy Reviews*, vol. 146, Aug. 2021, doi: 10.1016/j.rser.2021.111153.

[17] J. P. Hoffstaedt *et al.*, "Low-head pumped hydro storage: A review of applicable technologies for design, grid integration, control and modelling," *Renewable and Sustainable Energy Reviews*, vol. 158, Apr. 2022, doi: 10.1016/j.rser.2022.112119.

[18] I. Osman, D. Xiao, M. Rahman, M. Norambuena, and J. Rodriguez, "An optimal reduced-control-set model predictive flux control for 3L-NPC fed induction motor drive," *IEEE Transactions on Energy Conversion*, vol. 36, no. 4, pp. 2967–2976, Dec. 2021, doi: 10.1109/TEC.2021.3065373.

[19] D. Krishna, M. Sasikala, and V. Ganesh, "Mathematical modeling and simulation of UPQC in distributed power systems," in *2017 IEEE International Conference on Electrical, Instrumentation and Communication Engineering (ICEICE)*, Apr. 2017, pp. 1–5, doi: 10.1109/ICEICE.2017.8191886.

[20] D. Krishna, M. Sasikala, and R. Kiranmayi, "FOPI and FOFL controller based UPQC for mitigation of power quality problems in distribution power system," *Journal of Electrical Engineering and Technology*, vol. 17, no. 3, pp. 1543–1554, May 2022, doi: 10.1007/s42835-022-00996-6.

[21] D. Krishna, M. Sasikala, and V. Ganesh, "Adaptive FLC-based UPQC in distribution power systems for power quality problems," *International Journal of Ambient Energy*, vol. 43, no. 1, pp. 1719–1729, Dec. 2022, doi: 10.1080/01430750.2020.1722232.

[22] S. Krim, Y. Krim, and M. F. Mimouni, "Sensorless direct torque control based on nonlinear integral sliding mode controllers for an induction motor drive: Experimental verification," *Proceedings of the Institution of Mechanical Engineers, Part I: Journal of Systems and Control Engineering*, vol. 235, no. 2, pp. 249–268, Feb. 2021, doi: 10.1177/0959651820933733.

[23] S. Mahfoud, A. Derouich, N. EL Ouanjli, M. EL Mahfoud, and M. Taoussi, "A new strategy-based PID controller optimized by genetic algorithm for DTC of the doubly fed induction motor," *Systems*, vol. 9, no. 2, May 2021, doi: 10.3390/systems9020037.

[24] D. Krishna, M. Sasikala, and V. Ganesh, "Fractional order PI based UPQC for improvement of power quality in distribution power system," *International Journal of Innovative Technology and Exploring Engineering (IJITEE)*, vol. 8, no. 7, pp. 322–327, 2019.

[25] A. Mohan, M. Khalid, and A. C. Binojkumar, "Performance analysis of permanent magnet synchronous motor under DTC and space vector-based DTC schemes with MTPA control," in *2021 International Conference on Communication, Control and Information Sciences (ICCISc)*, Jun. 2021, pp. 1–8, doi: 10.1109/ICCISc52257.2021.9484869.

BIOGRAPHIES OF AUTHORS

Geeta Kamalapur received the B.E degree in Electrical and Electronics Engineering from Poojya Doddappa Appa College of engineering, Kalaburagi, Karnataka in 2011 and M. tech degree in Power Electronics from Poojya Doddappa Appa College of engineering, Kalaburagi, Karnataka in 2016. Currently she is an Assistant Professor at the Department Electrical and Electronics Engineering Sharnbasva University, Kalaburgi, Karnataka. Her research interest includes power electronics, electrical drives, electrical machines, direct torque control, harmonics distortion and ripple reduction. She can be contacted at email: geeta.u.kamalapur@gmail.com.

Mruttanjaya S. Aspalli currently working as professor and the course coordinator for M. Tech Power Electronics at Department of Electrical and Electronics Engineering, Poojya Doddappa Appa College of Engineering, Kalburagi, Karnataka, India and an Autonomous Institution. I have published 79 papers in national and international journals and conferences which are in the field of power electronics. His fields of interest are non-conventional energy (solar PV, wind): power conditioning, maximum power point tracking, stand-alone and grid connected systems. design of converters for renewable sources integrations, power quality and its related issues, power electronics and drives. He can be contacted at email: maspalli@gmail.com.